Proceedings of the 4th Jagiellonian Symposium on Advances in Particle Physics and Medicine

Mirror Matter Searches with the J-PET Detector

E. Pérez del Río[a,b,*], W. Krzemień[c] and B. Kłósek[d]
for the J-PET Collaboration

[a] *Faculty of Physics, Astronomy and Applied Computer Science, Jagiellonian University, 30-348 Kraków, Poland*
[b] *Centre for Theranostics, Jagiellonian University, 31-501 Kraków, Poland*
[c] *High Energy Physics Division, National Centre for Nuclear Research, 05-400 Otwock-Świerk, Poland*
[d] *Faculty of Mathematics and Computer Science, Jagiellonian University, 30-348 Kraków, Poland*

Doi: 10.12693/APhysPolA.142.386 *e-mail: elena.rio@uj.edu.pl

The positronium system — a bound state of an electron and a positron — is suitable for testing the predictions of quantum electrodynamics, since its properties can be perturbatively calculated to high accuracy and, unlike the hydrogen system, it is not affected by the finite size or quantum chromodynamics effects at the current level of experimental precision. Experiments searching for invisible decays of the positronium triplet state — the ortho-positronium — which mainly decays to three photons, are being conducted since they are sensitive to new physics scenarios, e.g., mirror matter, milli-charged particles, and extra space-time dimensions. The particular case of mirror matter and its search with the novel total-body positron emission tomography scanner at the Jagiellonian University is presented. This J-PET is a large, high precision medical imaging tool based on plastic scintillators.

topics: J-PET (Jagiellonian-positron emission tomography scanner), positronium, dark matter, mirror matter, invisible decays

1. Introduction

The Standard Model (SM) of particle physics is the current and most successful framework, which describes our understanding of the world. However, despite its accurate predictions and great success, there remain unanswered questions. Among them is the very nature of dark matter (DM). As the name suggests direct observation of DM by means of the electromagnetic interaction is not possible, but, due to its mass, DM does interact gravitationally. Indeed, several astrophysical observations have been interpreted as indirect evidence of the DM existence [1–5], and a large range of candidates for DM have been proposed — those with masses between 10^{-22} eV and 10^{15} GeV, as well as primordial black holes [6]. Many laboratory-based searches have been performed to detect DM particles [7–10]. But, so far, no experimental evidence has been found.

Mirror matter (MM) was originally proposed to restore parity violation in weak interactions by introducing a new hidden mirror sector where parity is violated in the opposite way. This means that under certain spatial inversion, the particles transform into a parity reflected new mirror state. These mirror partners would interact with SM particles via gravitation, making them suitable candidates for dark matter. In the ortho-positronium (oPs) system, the photons from the decay would oscillate into their mirror partners, leaving no signal in the detector. By performing a high precision measurement of the oPs lifetime, the accuracy of the present quantum electrodynamics (QED) calculations can be tested, and a search for the invisible decays of the oPs conducted. A discrepancy with the expectation from theory could indicate the presence of physics beyond the SM, i.e., a signal for MM.

2. The J-PET Detector

The J-PET (Jagiellonian positron emission tomography scanner) is a high acceptance multipurpose detector optimized for the detection of photons from positron–electron annihilation [11–13]. The device was built in two stages. The first one is the barrel detector, which is made of plastic scintillators. The barrel prototype is built from three cylindrical layers (radius of 42.5, length of 50 cm) [14]. Light signals from each strip are converted to electrical signals by photomultipliers placed at opposite ends of the strip [15–17]. This setup is completed with a newer, modular design, which can be recombined in several arrangements and added to the original detector configuration.

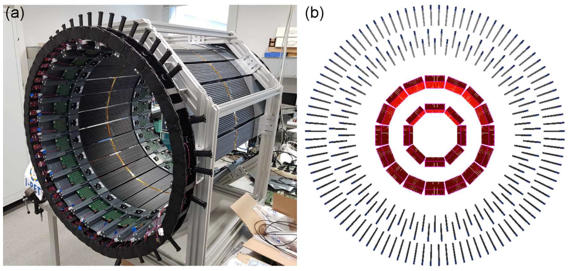

Fig. 1. (a) The fourth layer of the J-PET detector. (b) J-PET detector scheme with modules from the 4th layer rearranged into 2 internal layers.

This newer detector layer (see Fig. 1b) is read by matrices of silicon photomultipliers (SiPM), and it is expected to triple the efficiency of the single photon detection and improve the time resolution by about a factor of 1.5 [18].

The J-PET detector profits from very good timing resolution [18], the possibility of data taking in the continuous mode (triggerless) [19, 20], fully digital front-end electronics [21], and efficient discrimination between different positronium (Ps) decay channels [22]. This makes this tomography scanner not only suitable for medical purposes, but also advantageous in a broad scope of fields, e.g., medical imaging [23, 24], fundamental symmetry tests [25, 26], and quantum entanglement studies with oPs [27].

3. The mirror matter model and current status

Originally proposed by Lee and Yang [28], the concept of MM was introduced to restore spatial parity, which is known to be violated in weak interactions [29, 30]. Particularly, said authors suggested that each component of the ordinary matter would have a parity reflected partner. Further on, the idea was developed into MM models, introducing a hidden mirror sector, which would include not only the new particles but also interactions [31, 32]. In one particular case, not only gravity will govern the MM particles, but they would also interact with ordinary matter via a mixing mechanism, as proposed by S.L. Glashow [33]. In this model, the oPs decay can proceed via annihilation into a virtual single-photon. The virtual photon would oscillate into a mirror photon, connecting in this way the oPs with its correspondent mirror partner, oPs$'$, via the kinetic term

$$\mathcal{L} = \epsilon\, F^{\mu\nu} F^{'}_{\mu\nu}, \tag{1}$$

where ϵ, $F^{\mu\nu}$, and $F^{'}_{\mu\nu}$ are the mixing parameter, and field tensors for electromagnetism and mirror electromagnetism, respectively [33]. Values of ϵ can be constrained by the prediction of the primordial ^{4}He abundance by the SM, leading to $\epsilon \leq 3\times 10^{-8}$ [34], or be constrained by DM models [35]. In the latter case, one expects ϵ between $\sim 10^{-10}$ and $\sim 4\times 10^{-9}$, which corresponds to branching ratio expectations[†1] between 5×10^{-10} and 2×10^{-7}.

The search for such a particles can be carried out in the so-called invisible decays of positronium (Ps). Experimentally, this process would increase the observed oPs decay rate. Being a purely leptonic system, Ps is precisely described within the non-relativistic QED (NRQED) framework with very small radiative corrections from quantum chromodynamics (QCD) and weak interaction effects [36]. The most accurate measurements of the oPs decay rate are consistent with each other and with the theoretical prediction known up to two-loop ($\mathcal{O}(\alpha^2)$) corrections (see [36]).

The Tokyo group [37] obtained

$$\Gamma = \left(7.0401 \pm 0.0007\right) \times 10^6\,\mathrm{s} \tag{2}$$

with the oPs produced in SiO_2 powder, whereas Ann Arbor group [38] measured

$$\Gamma = \left(7.0404 \pm 0.0010_{(\mathrm{stat.})} \pm 0.0008_{(\mathrm{sys.})}\right) \times 10^6\,\mathrm{s} \tag{3}$$

with a slow positron beam on silica target. Despite the consistency of these results with the QED theory predictions, the present experimental uncertainties on the decay rate are about 100 times larger than the theoretical error, not reaching the needed sensitivity to test the oPs mirror component.

Previous searches for invisible decays have been performed by looking for an enhancement of events in a region where no signal from ordinary processes is expected. So far, the best limit set for the branching ratio BR of the oPs $\to$ *invisible* in vacuum has been delivered by the ETH Zürich group [39] at the confidence level of 90%. This best limit corresponds to

$$\mathrm{BR}\left(\mathrm{o-Ps} \to \mathrm{invisible}\right) < 3.0\times 10^{-5}, \tag{4}$$

which can be interpreted as a constraint on the mixing parameter $\epsilon < 5.0\times 10^{-8}$.

4. Mirror matter with the J-PET detector

As broadly discussed in [40], we intend to perform a precise measurement of the lifetime of the oPs, by means of its decay to 3-γ's (annihilation γ's) and compare it to the theoretical QED predictions. Any significant discrepancy between prediction and experiment would point in the direction of new physics, and under the frame of MM models, it would allow setting limits to the oPs $\to$ oPs$'$ $\to$ *invisible* process. For this purpose, we will use a 1 MBq ^{22}Na source, which decays through β^+ transitions, emitting a positron. The positron then undergoes free annihilation or forms positronium. In the J-PET, an amberlite coated chamber is placed

[†1] These calculations do not consider incoherent processes (e.g., collisions with matter) and thus apply only to oPs decays in vacuum.

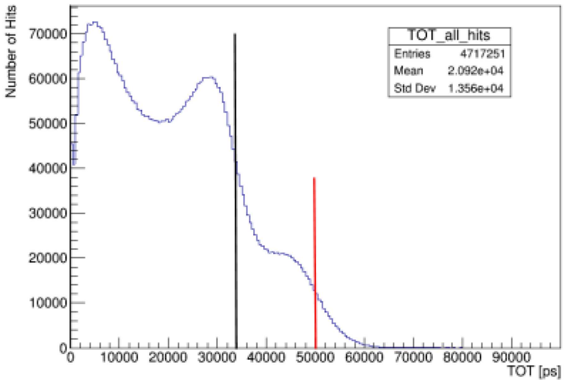

Fig. 2. Exemplary TOT spectra from Run 9 using all hits registered in the detector. The vertical black line shows the position of the annihilation Compton edge, while the red one represents the corresponding edge for the de-excitation photon.

surrounding the chamber, where the yield of 3-γ decays is increased [41]. Additionally, after a few picoseconds from the β^+ decay, a monochromatic photon — de-excitation photon — of 1.27 MeV is emitted by the excited nucleus. This allows for the setup of a reference time for the lifetime measurement. The main source of background to be considered is due to interactions with the surrounding matter — the pick-off process — which will decrease the relative ratio of 3-γ/2-γ annihilation.

In the J-PET detector, the photons can be identified using the time-over-threshold (TOT) technique. In Fig. 2, we can see the TOT spectra from the experiment. This quantity relates directly to the energy deposited via Compton interaction, where one can identify the Compton edges for annihilation and de-excitation candidates. We select exactly four photon candidates, including a de-excitation one, in order to build the lifetime distribution.

As mentioned previously, the ratio of 2-γ to 3-γ events can be altered due to the presence of background, originating from pick-off events. In order to reduce this spurious component of the lifetime and achieve the required sample purity, we make use of deep neural network (DNN) models for the classification of various background configuration types. An event is characterized by the set of features, including simple ones, such as hit positions and registration times, as well as complex ones, which combine the simple features into new representations taking into account the knowledge about the physical process, e.g., relative sum and difference of the relative annihilation photon angles calculated in the decay plane. For example, Fig. 3 shows the energies of the different hit candidates in the event for (a) the pick-off process and (b) the 3-γ signal. We tested different neural network (NN) models, which vary by the feature selection, as well as by the internal architecture details, such as the number of layers, interconnection types, and hyperparameters

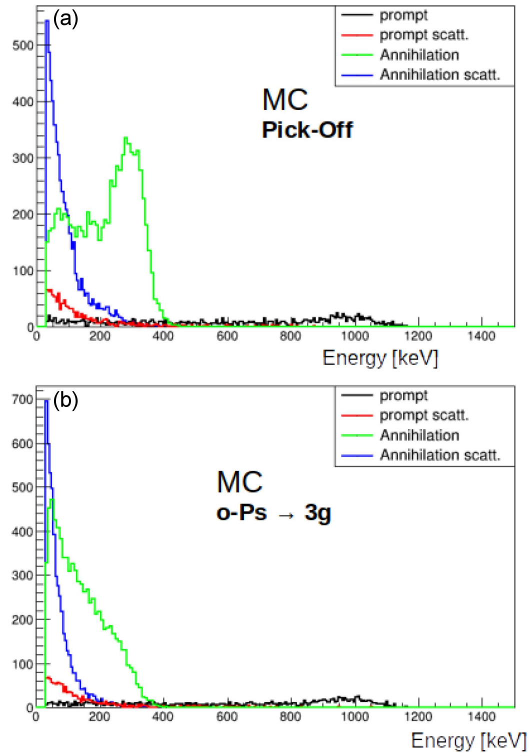

Fig. 3. (a) Simulated energies for the pick-off events: de-excitation (here *prompt*) photon without (black) and with (red) scattering in the detector and annihilation photon's energy without (green) and with (blue) scattering in the detector. (b) Simulated energies for the oPs signal events: energy of the de-excitation (*prompt*) photon without (black) and with (red) scattering in the detector and energy of the annihilation photons without (green) and with (blue) scattering in the detector.

values. The training, validation, and test phases are performed with the Geant4-based Monte Carlo simulation samples. The Monte Carlo model includes the physics of the decay and the detector response. We also tested different strategies, e.g., balanced vs unbalanced learning.

The preliminary results are very promising, e.g., a fully-connected four-layer NN (see Fig. 4) with nine input features achieved a test accuracy higher than 90%. This can be compared with the accuracy of the classifier corresponding to the typical topological selection cuts used in the current analyses, which on the same test set achieved a value of around 64%. The next steps involve the testing of the robustness of the classifier to the fluctuation of the relative frequency of the input classes, the tuning of the hyperparameters, and finalising the selection feature process. Finally, the classifiers should be tested against the experimental data samples.

The preliminary result of the background rejection, together with the J-PET achievable statistics of generated oPs, which amounts to $\approx 10^{13}$ after 2 years of data taking, and the efficiency for

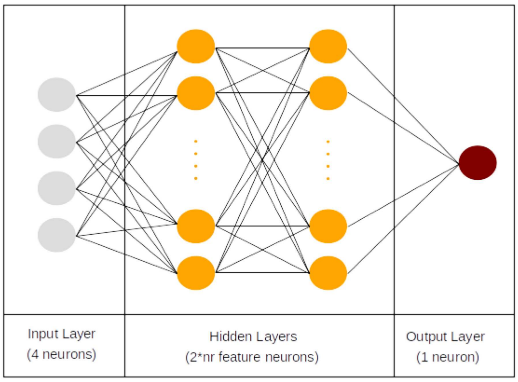

Fig. 4. DNN architecture used in the exploratory studies. The size of the hidden layers is determined by the number of features used in the network.

the detection of annihilation photons (2%) and of the de-excitation photon (about 20%) [23], together with the double-layered configuration, a sensitivity below 10^{-5} could be reached, improving the present best experimental accuracy of lifetime measurement, corresponding to 10^{-4}.

5. Conclusions

We aim to perform a search for oPs invisible decays with the precise measurement of the oPs lifetime distribution using the J-PET detector. Under the hypothesis that the oPs decays to invisible via oscillations into its mirror counter-partner oPs′, a discrepancy in the decay rate between the measurement and the prediction would be observed. This interpretation would assume that the NRQED calculations, which involve some truncations of QED terms, are exact to this accuracy. The estimated statistical sensitivity below 10^{-5} can be largely improved by re-configuring the detector layers, which would further increase the detection efficiency. Currently, we have focused on the subtraction of the pick-off background by using a deep neural network trained, tested, and validated on MC-based simulations, with very good preliminary prospects for data purity.

Acknowledgments

The J-PET Collaboration acknowledges the support provided by the Foundation for Polish Science through the TEAMPOIR.04.04.00-00-4204/17 Program; the National Science Centre of Poland through grant nos. 2019/35/B/ST2/03562, 2020/38/E/ST2/00112, and 2021/42/A/ST2/00423; the Ministry of Education and Science through grant no. SPUB/SP/490528/2021; the Jagiellonian University via project no. CRP/0641.221.2020, as well as the SciMat and qLife Priority Research Area budgets under the program Excellence Initiative — Research University at the Jagiellonian University.

References

[1] B. Holdom, *Phys. Lett. B* **166**, 196 (1986).

[2] C. Boehm, P. Fayet, *Nucl. Phys. B* **683**, 219 (2004).

[3] P. Fayet. *Phys. Rev. D* **75**, 115017 (2007).

[4] M. Pospelov, A. Ritz, M.B. Voloshin, *Phys. Lett. B* **662**, 53 (2008).

[5] Y. Mambrini, arXiv:1012.0447 (2010).

[6] G. Bertone, T.M.P. Tait, *Nature* **562**, 7725 (2018).

[7] S. Abrahamyan, Z. Ahmed, K. Allada et al., *Phys. Rev. Lett.* **107**, 191804 (2011).

[8] J.P. Lees, V. Poireau, V. Tisserand et al., *Phys. Rev. Lett.* **108** 211801 (2012).

[9] J.R. Batley, G. Kalmus, C. Lazzeroni et al. (NA48/2 Collaboration), *Phys. Lett. B* **746**, 178 (2015).

[10] A. Anastasi, D. Babusci, M. Berlowski et al. (KLOE-2 Collaboration), *Phys.Lett. B* **784**, 336 (2018).

[11] P. Moskal, E. Stepien, *PET Clinics* **15**, 439 (2020).

[12] P. Moskal, P. Kowalski, R.Y. Shopa et al., *Phys. Med. Biol.* **66**, 175015 (2021).

[13] R.Y. Shopa, K. Klimaszewski, P. Kopka et al., *Med. Image Anal.* **73**, 102199 (2021).

[14] S. Niedzwiecki, P. Białas, C. Curceanu et al., *Acta Phys. Pol. B* **48**, 1567 (2017).

[15] P. Moskal, N. Zoń, T. Bednarski et al., *Nucl. Instrum. Methods A* **775**, 54 (2015).

[16] P. Moskal, S.Niedźwiecki, T. Bednarski et al., *Nucl. Instrum. Methods A* **764**, 317 (2014).

[17] L. Raczyński, P. Moskal, P. Kowalski et al., *Nucl. Instrum. Methods A* **764**, 186 (2014).

[18] P. Moskal, O. Rundel, D. Alfs et al., *Phys. Med. Biol.* **61**, 2025 (2016).

[19] G. Korcyl, D. Alfs, T. Bednarski et al., *Acta Phys. Pol. B* **47**, 491 (2016).

[20] G. Korcyl, P. Białas, C. Curceanu et al., *IEEE Trans. Med. Imaging* **37**, 2526 (2018).

[21] M. Pałka, P. Strzempek, G. Korcyl et al., *J. Instrum.* **12**, P08001 (2017).

[22] D. Kamińska, A. Gajos, E. Czerwiński et al., *Eur. Phys. J. C* **76**, 445 (2016).

[23] P. Moskal, D. Kisielewska, C. Curceanu et al., *Phys. Med. Biol.* **64**, 055017 (2019).

[24] P. Moskal, K. Dulski, Neha Chug et al., *Sci. Adv.* **7**, eabh4394 (2021).

[25] P. Moskal, D. Alfs, T. Bednarski et al., *Acta Phys. Pol. B* **47**, 509 (2016).

[26] P. Moskal, A. Gajos, M. Mohammed et al., *Nat. Commun.* **12**, 5658 (2021).

[27] P. Moskal, N. Krawczyk, B.C. Hiesmayr et al., *Eur. Phys. J. C* **78**, 970 (2018).

[28] T.D. Lee, C.N. Yang, *Phys. Rev.* **104**, 254 (1956).

[29] C.S. Wu, E. Ambler, R.W. Hayward, D.D. Hoppes, R.P. Hudson, *Phys. Rev.* **105**, 1413 (1956).

[30] R.L. Garwin, L. Lederman, R. Weinrich, *Phys. Rev.* **104**, 254 (1956).

[31] A. Salam, *Nuovo Cim.* **5**, 299 (1957).

[32] I.Y. Kobzarev, L.B. Okun, I.Y. Pomeranchuk, *Sov. J. Nucl. Phys.* **3**, 837 (1966).

[33] S.L. Glashow, *Phys. Lett. B* **167**, 35 (1986).

[34] E.D. Carlson, S.L. Glashow, *Phys. Lett. B* **193**, 168 (1987).

[35] R. Foot, *Phys. Lett. B* **789**, 592 (2019).

[36] S. Bass, *Acta Phys. Pol. B* **50**, 1319 (2019).

[37] Y. Kataoka, S. Asai, T. Kobayashi, *Phys. Lett. B* **671**, 219 (2009).

[38] R.S. Vallery, P.W. Zitzewitz, D.W. Gidley, *Phys. Rev. Lett.* **90**, 203402 (2003).

[39] C. Vigo, L. Gerchow, B. Radics, M. Raaijmakers, A. Rubbia, P. Crivelli, *Phys. Rev. Lett.* **124**, 101803 (2020).

[40] W. Krzemien, E. Pérez del Río, K. Kacprzak *Acta Phys. Pol. B* **51**, 165 (2020).

[41] B. Jasinska M. Gorgol, M. Wiertel et al., *Acta Phys. Pol. B* **47**, 453 (2016).